ELSEVIER

Journal of Alloys and Compounds 434–435 (2007) 36–39

Journal of ALLOYS AND COMPOUNDS

www.elsevier.com/locate/jallcom

Microhardness and devitrification studies of Al–TM–RE alloys

P. Rizzi *, L. Battezzati

Dipartimento di Chimica IFM, Centro di Eccellenza NIS, V. Giuria 9, 10125 Università di Torino, Italy

Available online 26 September 2006

Abstract

The $Al_{87}Ni_7MM_6$ amorphous alloy was studied in order to understand the role of the Misch Metal (MM) on the devitrification behaviour. Three calorimetric peaks were found in DSC measurements. The first one is related to the precipitation of Al nanocrystals. Cu, Fe and Zr were also added to the $Al_{87}Ni_7MM_6$ alloy ($Al_{85}Ni_7MM_6Fe_1Zr_{0.5}Cu_{0.5}$) in order to improve the stability of the glassy phase. Primary precipitation of an intermetallic during devitrification was then found.

The microhardness was measured at different devitrification steps and the results are compared with those collected for other $Al_{87}Ni_7RE_6$ alloys (with RE: La, Ce, Nd, Sm).

Keywords: Nanocrystalline Al; Microhardness; Amorphous metals; Devitrification behaviour

1. Introduction

Because of their attractive mechanical properties [1–4] Al–TM–RE alloys (TM: Transition Metal; RE: Rare Earth) have reached a large interest in the last years. The most interesting microstructure is formed by nanocrystals dispersed in an amorphous matrix. The size and number per unit volume of nanocrystals influence the mechanical properties of the materials, changing their hardness and the deformation mechanisms. Therefore, it is of interest to understand the evolution of the transformation mechanism leading to the formation of nanocrystals [5,6], in order to single out the microstructure associated with the best mechanical properties.

In this work, Misch Metal was used instead of a single rare earth element with the aim of outlining the influence of the mixture of rare earth elements on the devitrification behaviour, on the stability of the amorphous phase and on the mechanical properties. Addition of a few percent of Fe, Cu and Zr was made in order to improve the stability of the amorphous phase and the ease of nucleation of fine crystals.

2. Experimental

Master alloys were prepared by arc melting the pure elements in an argon atmosphere. The Misch Metal used has the following composition: 50 at.% Ce, 25 at.% La, 17 at.% Nd, 8 at.% Pr. High temperature differential scanning calorimetry (HTDSC) was employed to monitor the melting and solidification behaviour of the master alloys, using scanning rates of 10 K/min. Rapidly solidified ribbons were produced by melt spinning. The structure of the samples was checked by X-ray diffraction (XRD) using Co Kα radiation. The devitrification studies were performed by using a differential scanning calorimeter (DSC) both in scanning and in isothermal mode. Scanning electron microscopy (SEM) was used to study the microstructure of the master alloys and of the ribbons at various devitrification stages. Transmission electron microscopy (TEM) was used both in bright field and in high resolution mode (HRTEM) in order to check the microstructure of the as quenched samples, by using an electrochemical thinning of 5% HNO_3 and 95% methanol.

The Vickers hardness was determined by using 25 g load and the samples were prepared by heating as quenched ribbons up to the end of the transformation peaks. Before testing, the samples surfaces were grinded with very fine grade papers in order to obtain flat areas.

3. Results

Two compositions were studied in this work ($Al_{87}Ni_7MM_6$ and $Al_{85}Ni_7MM_6Fe_1Zr_{0.5}Cu_{0.5}$, with MM: Misch Metal) and compared with alloys of general composition $Al_{87}Ni_7RE_6$ (with RE: La, Ce, Nd, Sm) reported elsewhere [7–9].

The microstructure of the $Al_{87}Ni_7MM_6$ master alloy was studied by SEM and dendrites of $Al_{11}MM_3$ were found beside dendrites of Al_3Ni. The two phases are surrounded by a binary eutectic composed by Al and $Al_{11}MM_3$. The melting and subsequent solidification of the alloy was followed by using an high temperature DSC (HTDSC). The eutectic melting starts at 625 °C, followed by two signals plus a liquidus at 955 °C

* Corresponding author. Tel.: +39 011 6707565; fax: +39 011 6707855.
E-mail address: paola.rizzi@unito.it (P. Rizzi).

0925-8388/$ – see front matter © 2006 Elsevier B.V. All rights reserved.
doi:10.1016/j.jallcom.2006.08.186

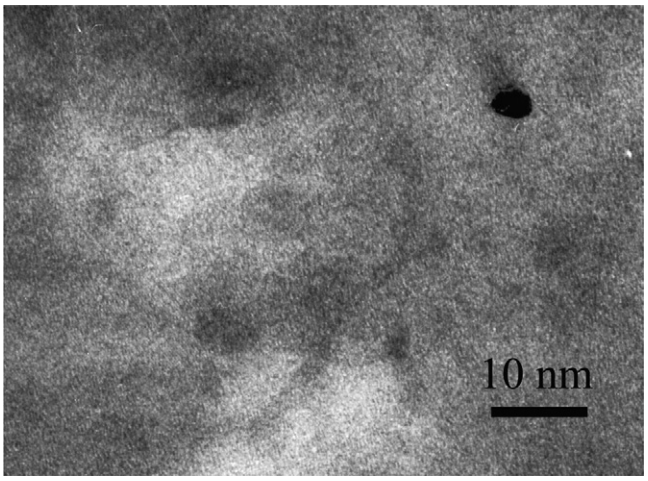

Fig. 1. HRTEM image of $Al_{87}Ni_7MM_6$ as quenched alloy, first preparation.

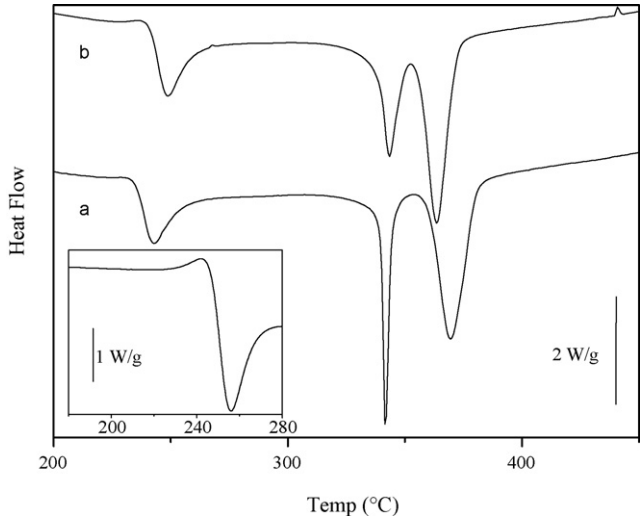

Fig. 2. DSC traces of $Al_{87}Ni_7MM_6$ with a scanning rate of 40 K/min: (a) first preparation; (b) second preparation. In the inset is shown a trace obtained with scanning rate of 80 K/min for the second preparation.

where melting ends. A large undercooling (about 90 °C) was registered for this alloy when the melt was cooled at 10 K/min in the HTDSC; in fact, $Al_{11}MM_3$ is the first phase that precipitates at 865 °C, followed at 774 °C by the solidification of Al_3Ni; the third signal observed is due to the change of structure of the phase $Al_{11}MM_3$ from the β-structure (Al_4Ba type) stable at high temperature to the α-structure (α-$Al_{11}La_3$ type) stable at low temperature. Also the eutectic was observed at lower temperature (616 °C) with respect to the melting curve.

The alloy was rapidly solidified in two preparations changing the solidification conditions, obtaining ribbons of about 80 and 50 μm thickness for the first and second preparation, respectively; this change in thickness can be associated with a change in solidification rate that is higher in the second preparation. Both ribbons result to be amorphous to an XRD analysis. TEM observations on the first sample revealed the presence of a limited number of fine crystals dispersed in the amorphous phase (see an example in Fig. 1). Thermal analysis was performed with the as quenched ribbons using the scanning rate of 40 K/min. The DSC traces, reported in Fig. 2, show slight differences between the two preparations, namely a change in the onset temperature of the first crystallisation process that pass from 233 °C (Fig. 2, curve a, first preparation) to 239 °C (Fig. 2, curve b, second preparation). For the second preparation (curve b) it is possible to note the presence of the glass transition temperature (T_g) immediately followed by the crystallisation process. T_g of the second preparation becomes more evident when the scanning rate is increased to 80 K/min as shown in the inset of Fig. 2. For the first preparation, T_g is less evident, even if a small endothermic signal is observed before crystallisation. The first DSC transformation is associated with the crystallisation of Al nanocrystals dispersed in the untransformed amorphous matrix. Two other transformation steps are detected at higher temperatures. The DSC peaks are different in height and width for the two preparations.

The $Al_{85}Ni_7MM_6Fe_1Zr_{0.5}Cu_{0.5}$ master alloy is constituted by dendrites of $Al_{11}MM_3$ surrounded by a ternary eutectic composed by Al, $Al_{11}Sm_3$ and Al_7Ni_2MM. For this composition an undercooling of about 30 °C is achieved during cooling of the melt at 10 K/min in an HTDSC and solidification of $Al_{11}MM_3$ start at 836 °C. The ternary eutectic melting starts at 625 °C and a few degrees of undercooling were observed during solidification.

Rapid solidification by melt spinning produces ribbons not completely amorphous as shown by XRD where a shoulder to the amorphous halo was detected at higher angles with respect to the maximum of the halo, in correspondence to the (2 0 0) Al peak. TEM observations on as quenched samples show the presence of crystals (Fig. 3) of about 10 nm in size. Their electron diffraction is assigned to an intermetallic phase rich in rare earth elements, with a primitive cubic lattice and lattice parameter of 0.661 nm [10].

DSC scans with the as quenched ribbons were made in order to check the thermal stability of the amorphous phase. The first transformation, associated with the crystallisation of the

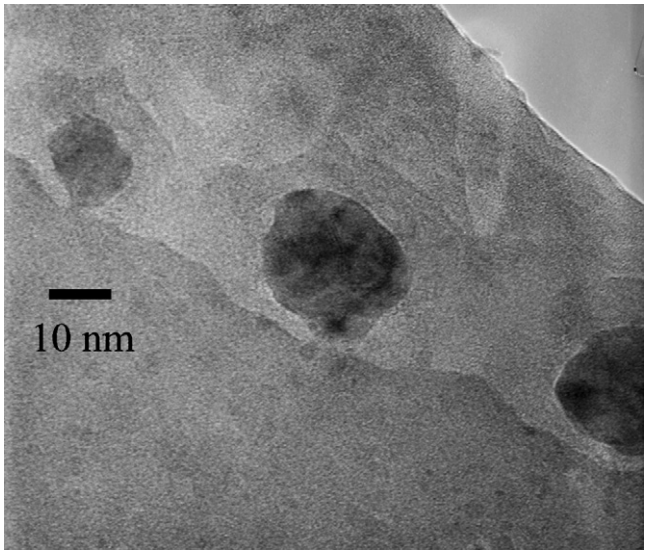

Fig. 3. HRTEM image of $Al_{85}Ni_7MM_6Fe_1Zr_{0.5}Cu_{0.5}$ as quenched alloy.

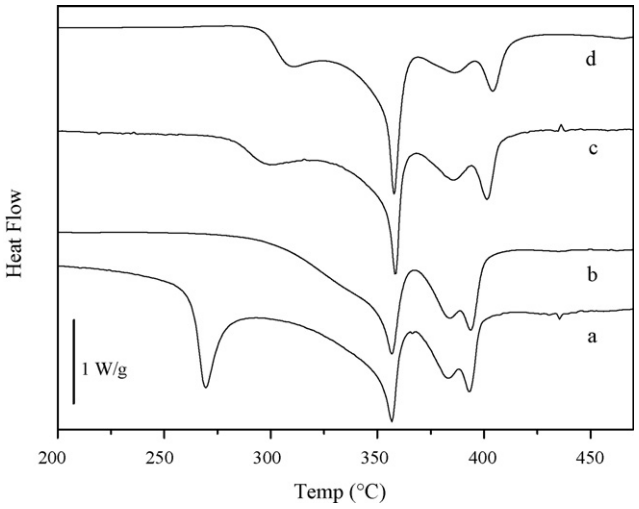

Fig. 4. DSC traces of $Al_{85}Ni_7MM_6Fe_1Zr_{0.5}Cu_{0.5}$: (a) as quenched; (b) scan after preanneling up to 300 °C; (c) scan after isothermal heating at 250 °C for 5 min; (d) scan after isothermal heating at 250 °C for 60 min.

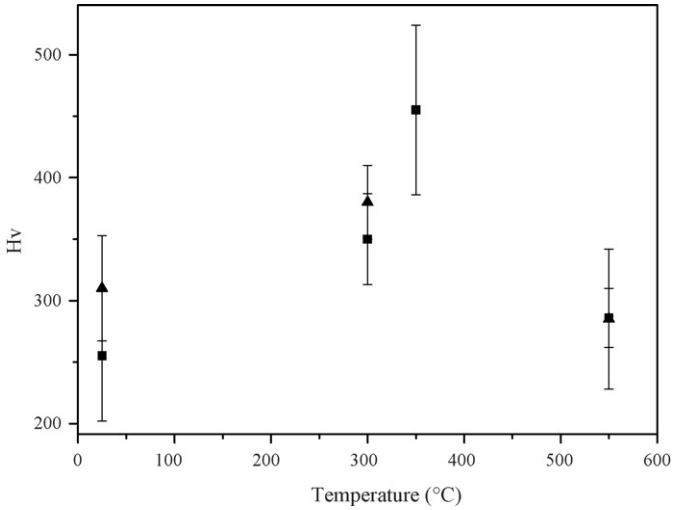

Fig. 5. Microhardness data for $Al_{85}Ni_7MM_6Fe_1Zr_{0.5}Cu_{0.5}$ (triangles points) and $Al_{87}Ni_7MM_6$ (squares) as a function of the temperature reached in DSC scans.

intermetallic phase described before, starts at 262 °C when the scanning is performed at 40 K/min and no evidence of T_g is found in this case (Fig. 4, curve a). The shape of the first calorimetric peak is slightly different from that of $Al_{87}Ni_7MM_6$ being narrower and steeper. Three other transformation steps were observed at higher temperatures.

Isothermal anneals were made with $Al_{85}Ni_7MM_6Fe_1Zr_{0.5}Cu_{0.5}$ samples at 250 °C, i.e. at lower temperature with respect to the onset of the primary crystallisation. In Fig. 4 (curves c and d) are reported the DSC scans performed with samples after the anneal. As the anneal time is increased, the onset temperature of the first peak shifts to higher temperatures and decreases in area. The other three transformation peaks are also displaced to higher temperatures with respect to the as quenched samples. If the ribbon is continuously heated up to 300 °C in DSC (i.e. at the end of the first transformation, Fig. 4, curve b) no change is observed in the subsequent calorimetric peaks at higher temperatures, that remain unchanged in area and in onset temperatures. Therefore, a different transformation path is acting if the anneal is done in isothermal or in scanning conditions. This is a quite unusual behaviour, not observed, for example, in the case of the $Al_{87}Ni_7MM_6$ alloy for which the production the nano-Al crystallisation does not influence the subsequent transformations. This effect is due to the precipitation of Al together with the metastable intermetallic phase when the annealing is isothermic. The precipitation stabilises the amorphous matrix remained untransformed and, as a consequence, produces a shift of the DSC peaks. The crystallisation of Al was not observed when heating up to 300 °C (at the end of the first transformation) was performed.

Microhardness measurements were performed on samples heated up to the end of the transformation peaks. The as quenched samples have Vickers hardness of 255 and 310 Hv for $Al_{87}Ni_7MM_6$ and $Al_{85}Ni_7MM_6Fe_1Zr_{0.5}Cu_{0.5}$, respectively (Fig. 5), values that increase when nanocrystals precipitate from the amorphous phase (350 and 380 Hv for $Al_{87}Ni_7MM_6$ and $Al_{85}Ni_7MM_6Fe_1Zr_{0.5}Cu_{0.5}$, respectively, heated up to 300 °C). A further increase was found after the second crystallisation peak for the $Al_{87}Ni_7MM_6$ alloy, reaching an hardness value of 455 Hv. Then a reduction in hardness occurs when the stable crystalline phases are formed. The higher value observed for the $Al_{85}Ni_7MM_6Fe_1Zr_{0.5}Cu_{0.5}$ can be explained referring to the microstructure of the as quenched samples described before. In fact, the rapidly quenched $Al_{85}Ni_7MM_6Fe_1Zr_{0.5}Cu_{0.5}$ already contains nanocrystals dispersed in the amorphous matrix; on the contrary a lower number of nanocrystals are formed in the other alloy.

Microhardness measurements were performed on $Al_{85}Ni_7MM_6Fe_1Zr_{0.5}Cu_{0.5}$ samples isothermally annealed at the temperature of 250 °C for 5 min and for 30 min. As already described before, after isothermal treatments intermetallic nanocrystals besides Al are observed. After 5 min of annealing, a value of 405 ± 20 Hv was found, that slightly decreases when the treatment is prolonged to 30 min (370 ± 20 Hv). This behaviour can be related to a change in volume fraction of nanocrystals present in the material which can be inferred from the DSC scans made after the isothermal treatments (Fig. 4, curves c and d). In fact, the area of the peaks is related to the amount of transformation produced during annealing and a progressive reduction in area with respect to the fully amorphous ribbons means increased crystallised fraction. A maximum in hardness values after 5 min of annealing indicates that the material with the most attractive mechanical properties is not obtained by heating the alloy up to the end of the transformation but by performing suitable isothermal treatments.

4. Discussion

$Al_{87}Ni_7MM_6$ is a multicomponent alloy because of the presence of the Misch Metal. The composition of the alloy is actually $Al_{87}Ni_7Ce_3La_{1.5}Nd_1Pr_{0.5}$. Because of the presence of Ce and La as majority elements it would be expected a devitrification behaviour similar to $Al_{87}Ni_7Ce_6$ and $Al_{87}Ni_7La_6$ that have two

transformations from the amorphous phase to the stable crystals. On the contrary, three crystallisation peaks were detected during devitrification, behaviour similar to the $Al_{87}Ni_7Nd_6$ alloy. Moreover, the stability of the glassy phase is decreased of about 10 degrees with respect to the ternary compositions containing Nd and about 20 °C with respect to that containing Ce. As already observed [8], the dimension of the RE atoms used in the $Al_{87}Ni_7RE_6$ alloys influence the stability of the amorphous phase and its devitrification behaviour. In particular, the glass forming ability is reduced decreasing the size of the elements (going from La to Nd) and the number of transformation peaks during devitrification pass from two (La, Ce, larger atoms) to three (Nd, Sm, smaller atoms). The use of the mixture of rare earth elements in the $Al_{87}Ni_7MM_6$ alloy produces an amorphous phase with a glass forming ability and devitrification tendency similar to that of the ternary alloys containing the smaller atoms (Nd, Sm), even if the average size of the RE used is more or less that of the Ce.

When a few percent of Fe, Cu and Zr are added to the $Al_{87}Ni_7MM_6$ alloy substituting for Al, a more complex devitrification path is observed, with the splitting of the last transformation DSC peak in two separated events. There is also an increment in the stability of the amorphous phase with onset temperature shifted to higher temperatures of about 20 °C with respect to the second $Al_{87}Ni_7MM_6$ preparation and the primary phase change from Al to an intermetallic phase.

The microhardness measurements performed in this work were compared with results on $Al_{87}Ni_7RE_6$ alloys (RE: La, Ce, Nd, Sm) showing similar trends at the different devitrification stages. The as quenched amorphous alloys have microhardness values around 280 Hv, that increases when nanocrystals are dispersed in the glassy matrix, reaching values of the order of 350 Hv, independently on the kind of nanocrystals produced (i.e. Al or intermetallics). Further increase can be obtained when three transformation steps characterise the amorphous alloy, obtaining values of about 500 Hv: at this stage the alloy is completely crystallised and constituted by a fine dispersion of intermetallics plus Al and the material is highly brittle. Then, when the stable crystalline phases are produced, a decrease in hardness is detected because of the increment in size of the grains constituting the materials, i.e. larger grains cause lower hardness values and vice versa. All this suggests that for $Al_{87}Ni_7RE_6$ alloys hardness is almost independent from the specific rare earth used but depends on the microstructure of the alloys, on the size of the crystals precipitated at each devitrification stage and on the composition of the amorphous matrix.

5. Conclusions

Two alloys ($Al_{87}Ni_7MM_6$ and $Al_{85}Ni_7MM_6Fe_1Zr_{0.5}Cu_{0.5}$) were produced by rapid solidification in the amorphous state. The use of the Misch Metal in $Al_{87}Ni_7RE_6$ alloy produces a decrease of the glass forming tendency of the system and a decrease of the stability of the amorphous phase with respect to the alloys with one RE element. Therefore, the addition of a few percent of Fe, Zr and Cu helps in increasing the crystallisation temperatures, changing also the primary crystalline phase formed during devitrification process from Al to a metastable intermetallic phase.

The precipitation of Al nanocrystals beside the metastable intermetallic phase during isothermal annealing in $Al_{85}Ni_7MM_6Fe_1Zr_{0.5}Cu_{0.5}$ produces a shift of the last transformations during devitrification, which is not observed when heating up to the end of the first peak is performed because of the precipitation of the intermetallic phase only.

Microhardness of $Al_{87}Ni_7RE_6$ alloys mostly depends on the microstructure of the materials and is almost independent on the specific rare earth constituting the alloys.

References

[1] A. Inoue, Prog. Mater. Sci. 43 (1998) 365.
[2] A. Inoue, H. Kimura, J. Light Met. 1 (2001) 31.
[3] A.L. Greer, Mater. Sci. Eng. A304–A306 (2001) 68.
[4] G. Wilde, N. Boucharat, R.J. Hebert, H. Rosner, W.S. Tong, J.H. Perepezko, Adv. Eng. Mater. 5 (2003) 125.
[5] A.K. Gangopadhyay, T.K. Croat, K.F. Kelton, Acta Mater. 48 (2000) 4035.
[6] F.Q. Guo, S.J. Poon, G.J. Shiflet, Mater. Sci. Forum 331–337 (2000) 31.
[7] L. Battezzati, S. Pozzovivo, P. Rizzi, Mat. Trans. 43 (2002) 2593.
[8] L. Battezzati, P. Rizzi, V. Rontò, Mater. Sci. Eng. A 375–377 (2004) 927.
[9] L. Battezzati, M. Kusý, P. Rizzi, V. Rontó, J. Mater. Sci. 39 (2004) 1.
[10] V. Rontó, L. Battezzati, A.R. Yavari, M. Tonegaru, N. Lupu, G. Heunen, Scripta Mater. 50 (2004) 839.